

# Journal of Materials Chemistry B

Accepted Manuscript



This is an *Accepted Manuscript*, which has been through the Royal Society of Chemistry peer review process and has been accepted for publication.

*Accepted Manuscripts* are published online shortly after acceptance, before technical editing, formatting and proof reading. Using this free service, authors can make their results available to the community, in citable form, before we publish the edited article. We will replace this *Accepted Manuscript* with the edited and formatted *Advance Article* as soon as it is available.

You can find more information about *Accepted Manuscripts* in the [Information for Authors](#).

Please note that technical editing may introduce minor changes to the text and/or graphics, which may alter content. The journal's standard [Terms & Conditions](#) and the [Ethical guidelines](#) still apply. In no event shall the Royal Society of Chemistry be held responsible for any errors or omissions in this *Accepted Manuscript* or any consequences arising from the use of any information it contains.

**Biodegradable and Biocompatible Soy  
Protein/Polymer/Adhesive Sticky Nano-textured Interfacial  
Membranes for Prevention of Esca Fungi Invasion into  
Pruning Cuts and Wounds of Vines**

S. Sett<sup>1†</sup>, M.W. Lee<sup>1†</sup>, M. Weith<sup>1</sup>, B. Pourdeyhimi<sup>2</sup> and A.L. Yarin<sup>1,3\*</sup>

<sup>1</sup>Department of Mechanical and Industrial Engineering,

University of Illinois at Chicago,

842 W. Taylor St., Chicago IL 60607-7022, USA

<sup>2</sup>3427 The Nonwovens Institute, Box 8301,

North Carolina State University

Raleigh NC 27695-8301, USA

<sup>3</sup>College of Engineering, Korea University, Seoul, S. Korea

## Abstract

Adhesive biodegradable membranes (patches) for protection of pruned locations of plants from esca fungi attacks were developed using electrospun soy protein/polyvinyl

\* To whom correspondence should be addressed. E-mail: [ayarin@uic.edu](mailto:ayarin@uic.edu). Phone: +1(312) 996-3472. Fax: +1(312) 413-0447.

†Equal contribution.

alcohol and soy protein/polycaprolactone nanofibers. Several different water-soluble adhesives were either added directly to the electrospinning solutions, or electrospayed onto the as-spun nanofiber mats. The nanofibers were deposited onto a biodegradable rayon membrane, and are to be pressed to the pruned location on a plant. The pore size in the nanofiber mats is sufficient for physically blocking fungi penetration, while the outside rayon membrane provides sufficient mechanical support in handling prior to deposition on a plant. Diseases like Vine Decline are one of the most important cases where such remedy would be needed. It should be emphasized that these novel biodegradable and sticky patches are radically different from the ordinary electrospun ultra-filtration membranes. The normal and shear specific adhesive energy of the patches were measured, and the results show that they can withstand strong wind without being blown off. On the other hand, the patches possess a sufficient porosity for plant breathing.

## 1. Introduction

Vine Decline is a disease complex caused by fungi named esca. The infected vine rots at heart wood and develops tiger stripe on leaves and black measles on berries<sup>1,2</sup>. In most cases, the entire vineyard should be replanted because the spores are airborne, easily spread to other vines, and infect them predominantly through prune locations. This kind of wound-infected disease can be spread by rain, wind, insects and birds. It causes huge economic losses with yield reduction, and the number of cases have been increasing for decade. Esca disease was reported in most of vineyards in Europe<sup>3</sup>. It also became a

world-wide problem after the fatal disease spread to countries including Canada, US, New Zealand, etc<sup>4-6</sup>. Similar fungi-related diseases attack other plants. For example, from 1904 to 1940, US south chestnut forest had been devastated by ‘Chestnut blight’, one of top three plant diseases in the world. Most of young vines are infected by esca and decline through wounds. The sites exposed to the atmosphere, such as wounds or pruning cuts, are dangerous channels for the fungi invaders<sup>7</sup>. Until now, the best way to control the disease was to cut and burn the infected prune. A popular fungicide, sodium arsenite was often used to control the widespread attack of esca, but the fungicide has now been banned in many countries and the disease could be spread all around the world. Prune paste and wound dressing, e.g. wax, was used to compartment the exposed sites from the environment, but they also delay the wound closure or kill the plant tissues or cells. A new solution should be provided to prevent and manage vines from infections in an environmentally-friendly way.

Electrospun biodegradable nanofibers are widely used in biomedical applications<sup>8-11</sup>, as nanofibrous scaffolds for tissue generation and tissue engineering<sup>12-15</sup>, as well as for antibacterial drug delivery<sup>16-18</sup>. The large surface-to-volume ratio and porous structure of such nanofiber mats have determined their usage in the filtration industry, both as water filters<sup>19-22</sup> and as air filters<sup>23,24</sup>. Polyvinyl alcohol (PVA) and polycaprolactone (PCL) are two of the most widely used biodegradable synthetic polymers for these applications<sup>25-28</sup>. PCL is an inexpensive, FDA approved water insoluble polymer without any toxicity and with controllable degradation. Using PCL, nanofibrous scaffolds for cartilage tissue regeneration<sup>29</sup> and scaffold for bone tissue<sup>30</sup> have been developed. Microfiltration

membranes for filtration of yeast cell were prepared using a blend of PCL and PLLA (poly L-lactic acid)<sup>31</sup>.

Due to an increased awareness in the environmental issues, natural biodegradable biopolymers, also popularly called green materials, have been widely studied over the last decade. Biodegradable biopolymer-derived materials with mechanical properties similar to those of synthetic polymers and derived from plant proteins, like soy protein, starch, cellulose, lignin, zein and sericin have been studied<sup>32-35</sup>. In particular, soy protein is one of the cheapest and readily available biopolymers obtained as a byproduct of soy-derived biodiesel.

Biodegradable and biocompatible nanofiber mats can be formed to be selectively permeable to air and/or moisture, and can be a possible remedy against esca infection. In the present work, sticky biodegradable nanofiber patches have been developed for direct application on plant wound sites. Both water soluble (a blend of soy protein/PVA) and water insoluble (a blend of soy protein/PCL) nanofibers were electrospun onto biodegradable rayon pads. Additionally, these nanofibers were made sticky with non-toxic adhesives by either adding them to the electrospinning solution or by electrospraying them onto the as-prepared nanofiber mats. These sticky patches are ready to use as a non-chemical way of preventing plants against esca attack [Fig. 1(1)].

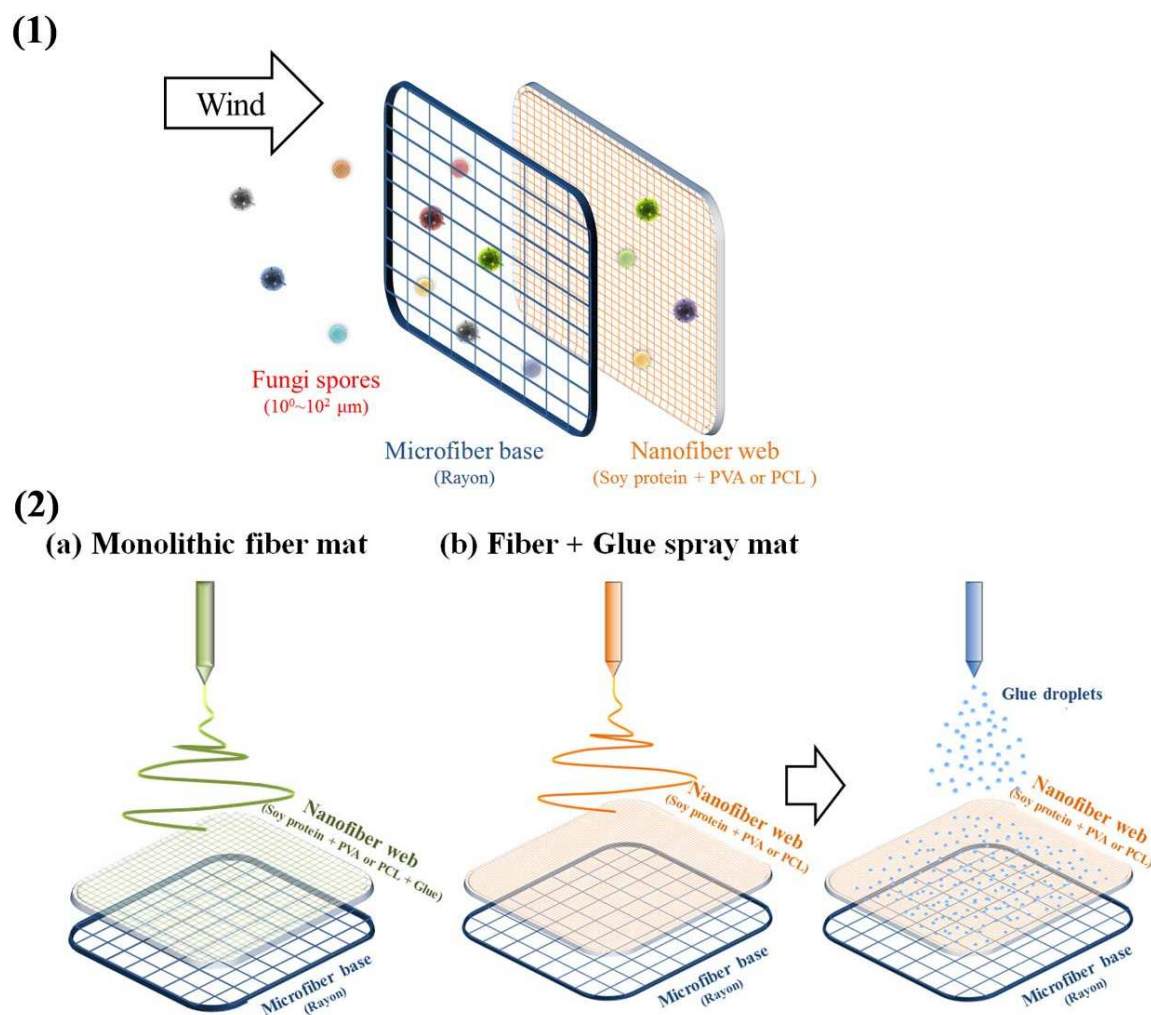


**Fig. 1.** (1) Functionality of the developed sticky green nano-textured patches. (2) Schematic of: (a) Monolithic fiber mat (PVA1-10, PVA2-10, PVA2-AD1-10, PVA2-AD3-10, PVA2-AD4-10, PCL1-10, PCL1-AD1-10, PCL1-AD310, PCL1-AD4-10) (b) Fiber electrospinning and adhesive electrospaying: Electrospaying Micronax 241-01(AD1) and repositionable (AD2) adhesive onto electrospun soy protein/PVA and soy protein/PCL nanofiber mats (SPv01, SPv02, SPc01, SPc02).

Peeling specific energy is an important characteristic of nanofiber applications as adhesives, which is foreseen in the present work. The specific energies discussed in the present manuscript are defined as the adhesion energy per unit interfacial area, with the units  $\text{J/m}^2 = \text{N/m}$  in the SI System of Units. The unit  $\text{N/m}$  also ascertains the fact that the specific adhesion energy can be considered as the surface tension. A number of different methods can be found for measuring the specific adhesive energy of nanofiber mats. Shear adhesion testing for dry adhesives are used for characterization of directionally-sensitive adhesives<sup>36</sup>. Shaft-loaded blister test is used for measuring debonding radius of electrospun fiber membranes<sup>37</sup>. Adhesive forces between electrospun polymer fibers have been tested using industry standard peeling tests<sup>38,39</sup>. In the present work peeling and shear tests will be used to examine adhesion the sticky green nano-textured patches.

## 2. Experimental

### 2.1 Materials

Polyvinyl alcohol (PVA,  $M_w = 130$  kDa, 99%+ hydrolyzed, and  $M_w = 9$  kDa, 80% hydrolyzed) and polycaprolactone (PCL,  $M_n = 80$  kDa) were obtained from Sigma Aldrich. Solvents, formic acid,  $M_w = 46.03$  Da, and acetic acid,  $M_w = 60.05$  Da, were obtained from Sigma Aldrich. Two different kinds of soy protein were used, one being water soluble, and the other one being water insoluble. Both water-soluble soy protein, Clarisoy<sup>TM</sup> 100, and water insoluble soy protein, Pro-Fam 955, were obtained from ADM

Specialty Food Ingredients. PVAc (Polyvinyl acetate) wood glue, water soluble adhesive SIMALFA 4574, repositionable glue, and pressure-sensitive adhesive Micronax 241-01 were obtained from Gamblin Artist's Colors, SIMALFA Water Borne Adhesives, Scaraperfect, and Franklin Adhesives, respectively. All adhesives are non-toxic in nature, with water-based Micronax 241-01 being FDA approved (compliant under 21CFR 175.105, 21CFR 176.170 and 21CFR 176.180). Non-ionic trislixane-(poly)ethoxylate surfactant SILWET L77 was generously donated by Momentive. Tucks medicated cooling pads were obtained from Johnson & Johnson. These cooling pads, made from biodegradable rayon (regenerated cellulose) fabric, were used as a substrate on which nano-textured nanofiber mats were deposited. The specific adhesive energy of the prepared samples were measured on wooden surfaces. For this, balsa wood strips obtained from McMaster-Carr were used as a model material.

## 2.2 Solution Preparation

Monolithic nanofibers of the two different types of soy protein were generated by electrospinning. For the water-soluble Clarisoy, the aqueous solutions were prepared as follows. To prepare homogeneous solution of soy protein/PVA with lower molecular weight PVA, water and ethanol mixture was used as a base solvent. At the beginning, 4.5 g each of deionized water and ethanol were mixed. Then, 2.5 g of PVA ( $M_w = 9$  kDa, 80% hydrolyzed) was added to this solution and left on a hot plate at 95 °C under constant stirring for 4 h. Then, 0.5 g of Clarisoy was added to the PVA solution and the

solution was left for 12 h at 80 °C under constant stirring resulting in the soy protein/PVA ratio of 16.7/83.3 (w/w). This solution was labelled as solution PVA1.

The adhesive solutions used for electrospaying were prepared as follows. FDA-approved Micronax adhesive (labelled AD1) was electrospayed as received. In parallel, 4.0 g of repositionable glue was dissolved in 5.0 g of water-ethanol mixture (80:20 w/w) and stirred at 50 °C for 2 h. This solution was labelled as solution AD2.

Using higher molecular weight PVA, blends of PVA ( $M_w = 130$  kDa, 99%+ hydrolyzed), Clarisoy and different adhesives in water were used. First, 7.5% PVA solution was prepared by mixing 0.75 g of PVA with 9.25 g of deionized water and left on a hot plate at 95 °C under vigorous stirring for 4 h. Separately, 10% water-soluble soy protein solution was prepared by mixing 1 g of Clarisoy with 9 g of deionized water and left at 60 °C under constant stirring for 24 h. After the solutions were cooled to room temperature, 2.5 g of 10% water-soluble soy protein solution was added to 5 g of 7.5% PVA, resulting in the soy protein/PVA ratio of 40/60 (w/w). This solution was labelled as solution PVA2. Then, three different adhesives were added to solution PVA2. Namely, 1 g each of PVAc wood glue, SIMALFA 4574, and Micronax 241-01 were added to three separate solutions of PVA2 and the resulting solutions were labelled as PVA2-AD3, PVA2-AD4, and PVA2-AD1, respectively. The mixture solutions were stirred at room temperature for 1 h. The solutions formed were homogeneous and there was no phase separation. Fully hydrolyzed PVA cannot be electrospun<sup>40,41</sup> and sporadic electrospaying of droplets is observed<sup>42</sup>. To obtain nanofibers, 0.0425 g (0.5% w/w) of non-ionic surfactant SILWET L77 was added to solutions PVA2-AD3, PVA2-AD4, and PVA2-AD1 and stirred for 5 min just before electrospinning.

Using water-insoluble soy protein, the solutions were prepared as follows. First, 15% PCL solution was prepared by mixing 1.5 g of PCL with 2.125 g of formic acid and 6.375 g of acetic acid (formic acid – acetic acid ratio of 25:75 v/v), and the solution was left for 24 h on a hot plate at 50 °C under constant stirring. Obtaining bead-free continuous soy protein/PCL nanofibers was difficult, while using formic acid as the only solvent. Hence, formic acid-acetic acid mixture solution was used for preparing PCL solutions<sup>43</sup>. Separately, 18% water-insoluble soy protein solution was prepared by mixing 1.8 g of water insoluble Pro-Fam 955 soy protein with 8.2 g of formic acid and left at 60 °C under constant stirring for 24 h. After the solutions were cooled to room temperature, 4.17 g of water-insoluble soy protein solution was added to 5 g of 15% PCL, resulting in the soy protein/PCL ratio of 50/50 (w/w). This solution was labelled as solution PCL1. Adhesive solutions AD1 and AD2 were used for electrospaying onto nanofibers electrospun from solution PCL1.

Similar to solution PVA2, three different adhesives were also added to solution PCL1. In particular, 1 g each of PVAc wood glue, SIMALFA 4574, and Micronax 241-01 were added to three separate solutions of PCL1 and the resulting solutions were labelled as PCL1-AD3, PCL1-AD4, and PCL1-AD1, respectively. The mixture solutions were stirred at room temperature for 1 h. The solutions formed were homogeneous and there was no phase separation.

Fibers could not be electrospun from solutions prepared by adding repositionable glue to either PVA-based PVA2 solution, or PCL-based PCL1 solution. Since the adhesive AD2 is gelatinous in nature, a proper homogeneous blend solution of the

adhesive with polymer and soy protein could not be formed. Due to this, electrospinning of soy protein/polymer solutions containing adhesive AD2 could not be conducted.

### 2.3 Electrospinning

Monolithic fibers of soy protein/PVA and adhesive/soy protein/PVA were prepared using a standard electrospinning setup. The electrospinning technique is described elsewhere<sup>8,9,44-48</sup>. Randomly oriented nanofibers of solutions PVA1, PVA2, PVA2-AD1, PVA2-AD3, and PVA2-AD4 were collected on the rayon pads kept on an aluminum foil for 10 min while keeping the flow rate at 0.3-0.5 mL/h. A 15-18 kV positive voltage was applied to the solutions and the distance between the tip of the needle and the rayon pad was about 10-15 cm while keeping the relative humidity at 30%. Electrospinning was done using 18 gauge needle, having the outer diameter of 1.27 mm and the inner diameter of 0.838 mm. Direct electrospinning of PCL-based solutions created fluffy nanofibers and caused delamination of the fiber mat from the rayon pad (described in details in the Results section). To prevent delamination and enhance adherence of the electrospun nanofiber mat to the rayon pad, adhesive was initially electrospayed at 0.5 mL/h and 15 kV positive voltage for 5 min onto bare rayon pads. The initial adhesive electrospayed was chosen to be the same as the adhesive in the respective solution used for electrospinning. Only for pure soy protein/PCL fibers, adhesive solution AD1 was used. This was done because among the four adhesives used this one possessed the minimum specific adhesive energy and is FDA approved. Immediately after electrospaying, electrospinning was conducted onto the pads for 10 min at a flow rate of 0.3-0.5 mL/h,

and a positive voltage of 14-16 kV was applied to the solutions. The distance between the tip of the needle and the substrate and the relative humidity were the same as for PVA-based solutions.

Electrospinning was conducted for 10 min for solutions PVA1, PVA2, PVA2-AD1, PVA2-AD3, and PVA2-AD4 and the samples were labelled as PVA1-10, PVA2-10, PVA2-AD1-10, PVA2-AD3-10, and PVA2-AD4-10, respectively. Additionally, to measure the dependence of the specific adhesive energy on electrospinning time, solution PVA2-AD3 was electrospun for 5 min, 10 min and 20 min onto separate rayon pads. Solutions PVA2-AD3 were chosen for this test because PVAc wood glue (AD3) was found to be the strongest among all the adhesives. These samples were labelled PVA2-AD3-5, PVA2-AD3-10 and PVA2-AD3-20. For electrospinning of soy protein/PCL fibers, the adhesive solution AD1 was initially electrospayed for 5 min, followed by electrospinning of solution PCL1 for 10 mins. This sample was labelled PCL1-10. Similarly, solutions AD1, AD3, and AD4 were electrospayed for 5 min followed by electrospinning of PCL1-AD1, PCL1-AD3, and PCL1-AD4 on the respective electrospayed rayon pads. These samples were labeled as PCL1-AD1-10, PCL1-AD3-10, and PCL1-AD4-10. To measure the dependence of the specific adhesive energy on electrospinning time, PCL-AD3 solution was electrospun onto the AD3-electrospayed rayon pad for 5 min, 10 min, and 20 min. The initial electrospaying time was kept constant at 5 min. These samples were labelled as PCL1-AD3-5, PCL1-AD3-10, and PCL1-AD3-20, respectively. Different samples prepared and their compositions are listed in Table 1.

**Table 1.** Composition of different samples prepared by electrospinning and electrospaying of adhesive solutions.

Sample	Polymer		Soy-protein		Adhesive		Time of spinning (min)	Avg. fiber diameter (nm)
	Type	Conc. (% wt in sol.)	Type	Conc. (% wt in sol.)	Type	Conc. (% wt in sol.)		
PVA1-10	PVA (9 kDa)	20.83	Clarisoy	4.17	None	None	10	713
PVA2-10	PVA (130 kDa)	5	Clarisoy	3.33	None	None	10	728
PVA2-AD1-10	PVA (130 kDa)	4.41	Clarisoy	2.94	Micronax	11.76	10	805
PVA2-AD3-5	PVA (130 kDa)	4.41	Clarisoy	2.94	PVAc	11.76	5	761
PVA2-AD3-10	PVA (130 kDa)	4.41	Clarisoy	2.94	PVAc	11.76	10	766
PVA2-AD3-20	PVA (130 kDa)	4.41	Clarisoy	2.94	PVAc	11.76	20	769
PVA2-AD4-10	PVA (130 kDa)	4.41	Clarisoy	2.94	Simalfa	11.76	10	782
SPv01	PVA (9 kDa)	20.83	Clarisoy	4.17	Micronax	Electro-spray	10	716
SPv02	PVA (9 kDa)	20.83	Clarisoy	4.17	Repositio-nable glue	Electro-spray	10	714
PCL1-10	PCL	8.18	Pro-Fam 955	8.18	None	None	10	987
PCL1-AD1-10	PCL	7.37	Pro-Fam 955	7.37	Micronax	9.83	10	1018
PCL1-AD3-5	PCL	7.37	Pro-Fam 955	7.37	PVAc	9.83	5	999
PCL1-AD3-10	PCL	7.37	Pro-Fam 955	7.37	PVAc	9.83	10	1004
PCL1-AD3-20	PCL	7.37	Pro-Fam 955	7.37	PVAc	9.83	20	1002
PCL1-	PCL	7.37	Pro-Fam	7.37	Simalfa	9.83	10	1009

AD4-10			955					
SPc01	PCL	8.18	Pro-Fam 955	8.18	Micronax	Electro- spray	10	1016
SPc02	PCL	8.18	Pro-Fam 955	8.18	Repositio -nable glue	Electro- spray	10	1015

#### 2.4 Electro spraying adhesive solutions onto soy protein/PVA and soy protein/PCL fiber mats

Adhesive solutions AD1 and AD2 were electro sprayed onto samples PVA1-10 and PCL1-10. Electro spraying of Micronax 241-01 (AD1) and repositionable glue (AD2) were conducted onto separate samples of PVA1-10 and PCL1-10 for 10 min and the samples with the adhesives were labelled as samples SPv01 and SPv02 for the soy/PVA fiber mats, and SPc01 and SPc02 for the soy/PCL fiber mats, respectively. The flow rate was maintained at 0.5 mL/h, and a 15 kV positive voltage was applied to the adhesive solutions. The distance between the tip of the needle and the mat was about 10 cm. It should be emphasized that for electro spraying repositionable glue (AD2), only adhesive droplets from the solution reached the nanofiber mat. For SPv02, both soy protein and PVA being water soluble, water droplets from adhesive reaching the nanofiber mat would have dissolved the polymer and the fiber structure would be destroyed. By controlling the electro spraying conditions (the applied voltage, flow rate and nozzle-to-ground distance), the nanofiber structure was kept intact after electro spraying the repositionable adhesive (AD2). This can be verified by the fact that only small adhesive droplets were seen on SPv02 samples after electro spraying, and one could conclude that water of the adhesive solution evaporated and did not reach the fiber mat. Such controlled conditions could not

be obtained for electrospaying of adhesive AD1, and samples SPv01 had large droplets after electrospaying. The entire water did not evaporate and some of it reached the fiber mat. The schematic of electrospaying adhesives is shown in Fig. 1 (2). The composition of the different samples prepared by electrospaying adhesives onto electrospun nanofiber mats are listed in Table 1.

### 2.5 180° peeling tests

The normal adhesion force of prepared nanofiber mats with adhesives was measured in mechanical peeling tests. In general, 1 kg of weight was gently rolled 20 times on a 6 cm x 2 cm sample placed on a balsa wood strip (10 cm x 2.6 cm) right after electrospinning. Then, a 180° peel test was performed using a 100 N capacity Instron machine (model 5942). The upper and lower ends of the samples were clamped by Instron's pneumatic grips. The upper end was stretched at a constant rate of 10 mm/min, while the lower end was kept at its initial position (Fig. 2a). The peeling tests were conducted until the entire sample was peeled off the balsa wood strip. For repositionable glue electrospayed onto nanofiber mat (samples SPv02 and SPc02), the same sample was pressed and the peeling test was done for several consecutive times. SPv02 was tested in this manner for 7 times. The stickiness of SPc02 was lost after three trials, and hence the latter sample could not be tested for more than 3 times. For pressure-sensitive Micronax adhesive samples (samples SPv01 and SPc01), the peeling test was conducted for different applied weights on samples, 1 kg, 5 kg, and 11.5 kg. Thus the pressure

applied to the samples changed from 0.83 kPa (for 1 kg) to 4.17 kPa (for 5 kg) and finally to a maximum of 9.55 kPa (for 11.5 kg).

## 2.6 Dead weight test

The specific shear adhesion energy was measured by ‘dead weight’ test, which is a standard test for measuring the specific adhesion energy of nanofiber mats<sup>35</sup>. A sample (2.3 cm x 5 cm) was adhered to the balsa wood strip by loading 1 kg weight for 1 min (Fig. 2b). The edge of sample was connected to an empty container through the pulley. After the weight had been removed, water was slowly poured into the container until the sample delaminated from the wooden strip. The specific shear adhesion energy was calculated from the total weight of water in the container when delamination occurred.

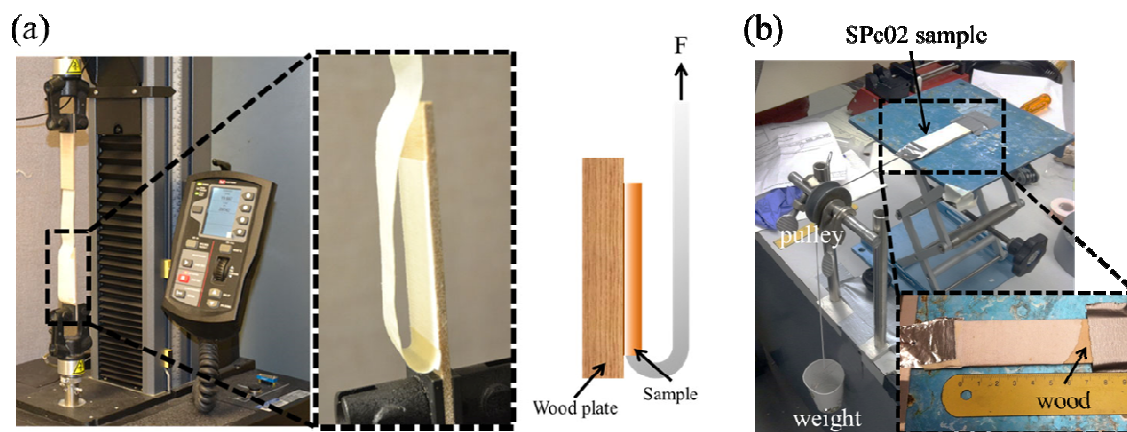


**Fig. 2.** (a) 180° peeling test of samples using Instron machine. (b) Dead weight test.

## 2.7 Optical characterization

All optical images were taken using optical microscope Olympus BX-51. SEM images and EDX analysis were obtained using Hitachi S-3000 N.

### 3. Results and Discussion

#### 3.1. Monolithic soy protein/PVA and soy protein/PCL nanofiber mats

Solutions PVA1, PVA2 and PCL1 were electrospun and the soy protein/PVA nanofibers are depicted in Fig. 3(1), whereas the soy protein/PCL nanofibers can be seen in Fig. 3(2) (both on rayon substrate). EDX spectra of these nanofibers were obtained to detect the presence of soy protein in the as-spun monolithic fibers. Soy protein contains sodium (Na), phosphorus (P), and sulfur (S) which are considered as its unique markers<sup>49</sup>. Figs. 4a, 4b and 4c show the EDX spectra of monolithic soy protein/PVA and soy protein/PCL nanofibers obtained by electrospinning solutions PVA1, PVA2 and PCL1, respectively. The percentage content of different elements is shown in Table 2 and the values are in good agreement with soy content in soy protein/nylon 6 fibers<sup>49</sup>. The weight % of Na, P and S is higher for the sample PVA2-10 than for the sample PVA1-10 as the soy protein/PVA ratio for the sample PVA2-10 is 40/60 (w/w) as compared to 16.7/83.3 (w/w) for the sample PVA1-10. Also, different soy proteins possess different contents of Na, P and S. Water-soluble Clarisoy has a higher percentage of Na as compared to P and S, whereas water-insoluble Pro-Fam 955 has a higher percentage of P and S as compared to Na (cf. Table 2).

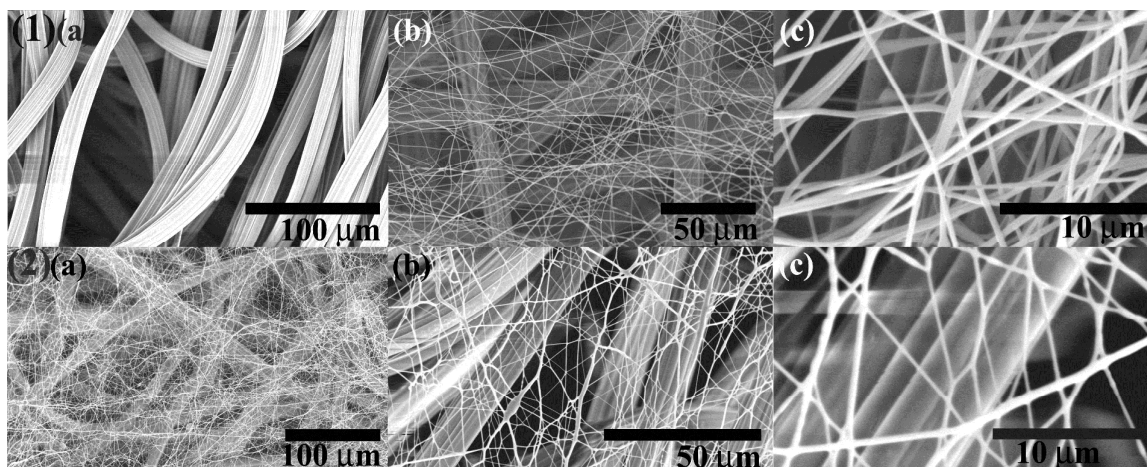


**Fig. 3.** (1) SEM images of: (a) Rayon substrate prior to nanofiber deposition. (b) Large rayon fiber strands of the substrate seen beneath the deposited soy protein/PVA fibers, and (c) The enlarged view of the deposited soy protein/PVA nanofibers of sample PVA2-10. (2) SEM images of soy protein/PCL nanofibers electrospun from solution PCL1. (a) & (b) Large rayon fiber strands of the substrate seen beneath the deposited soy protein/PCL fibers, and (c) The enlarged view of the deposited soy protein/PCL nanofibers of sample PCL1-10.

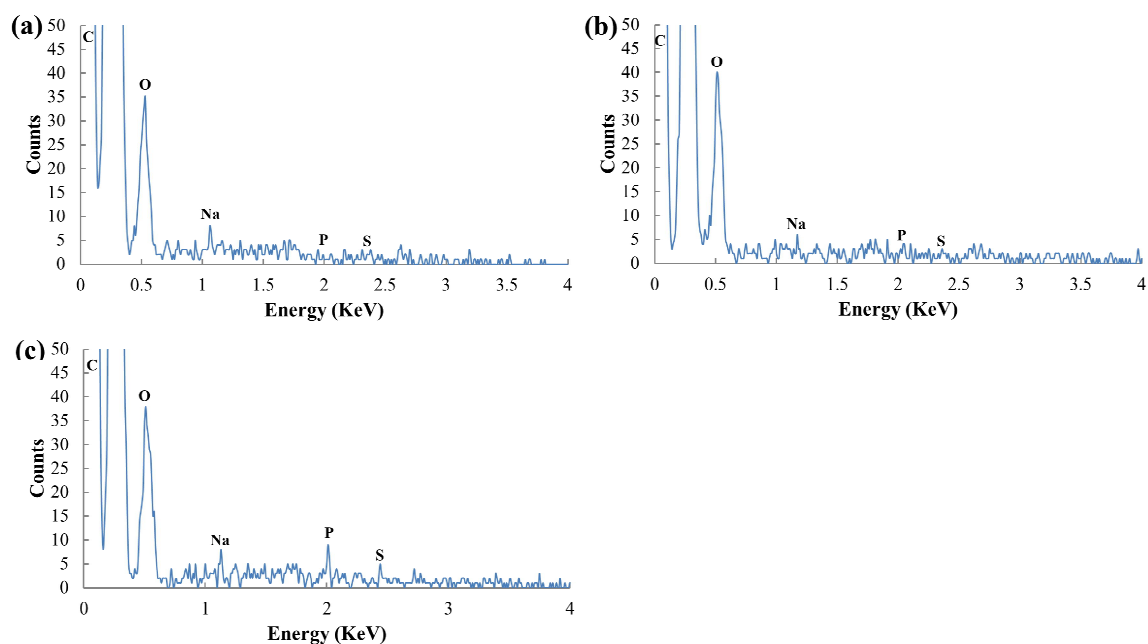


**Fig. 4.** EDX spectra of: (a) 16.7/83.3 soy protein/PVA nanofibers (sample PVA1-10), (b) 40/60 soy protein/PVA nanofibers (sample PVA2-10), and (c) 50/50 soy protein/PCL nanofibers (sample PCL1-10), all three samples on rayon pads.

**Table 2.** Element content in monolithic soy protein/PVA (samples PVA1 and PVA2) and soy protein/PCL (sample PCL1) nanofibers.

Element	Weight %		
	Sample PVA1-10	Sample PVA2-10	Sample PCL1-10
Carbon (C)	82.95	73.62	85.16
Oxygen (O)	16.67	25.55	14.18
Sodium (Na)	0.2	0.45	0.17
Phosphorus (P)	0.06	0.1	0.29
Sulfur (S)	0.13	0.28	0.20
Total	100.1	100.0	100.0

### 3.2 Electrospinning of water-soluble adhesive/soy protein/PVA and water-insoluble adhesive/soy protein/PCL solutions

#### 3.2.1 Normal specific adhesive energy of different fiber mats

Electrospun soy protein/PVA and soy protein/PCL fibers containing PVAc wood glue, samples PVA2-AD3-10 and PCL1-AD3-10, respectively, are shown in Fig. 5. The fiber morphology was not as uniform as it was for pure soy protein/PVA or pure soy

protein/PCL fibers electrospun from solutions PVA2 and PCL1. The electrospun fibers containing adhesives appeared beaded at different places along the fiber length due to the presence of the adhesives in solutions. However, the fiber distribution on the rayon mat was similar to the soy protein/PVA and soy protein/PCL fibers. Samples PVA2-AD1-10, PVA2-AD4-10, PCL1-AD1-10, and PCL4-AD1-10 possessed similar fiber morphology to that of the samples PVA2-AD3-10 and PCL1-AD3-10.

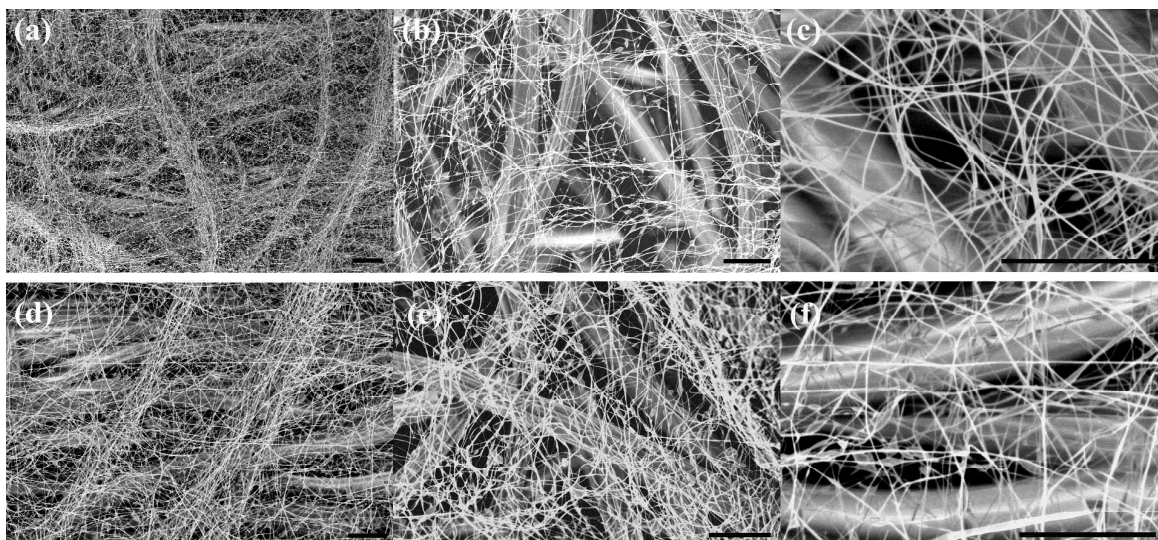


**Fig. 5.** Electrospun monolithic fibers on rayon pad. (a)-(c) PVA2-AD3-10, and (d)-(f) PCL1-AD3-10. The scale bars are 25  $\mu\text{m}$ .

Prior electrospaying of adhesives was required for PCL-based solutions. This is because the soy protein/PCL fibers or the adhesive/soy protein/PCL fibers were rather fluffy and did not reveal good adherence to rayon pads (Fig. 6b), unlike the adhesive/soy protein/PVA fibers. This also caused some delamination of the adhesive/soy protein/PCL fibers, where at the end of the peeling test, some of the electrospun adhesive/soy

protein/PCL fibers delaminated from the rayon pad and stuck to the balsa wood strip (Fig. 6a). This delamination effect was observed irrespective of the adhesive used. To avoid delamination, adhesive was first electrospayed on bare rayon pad for 5 min as described in the experimental section.

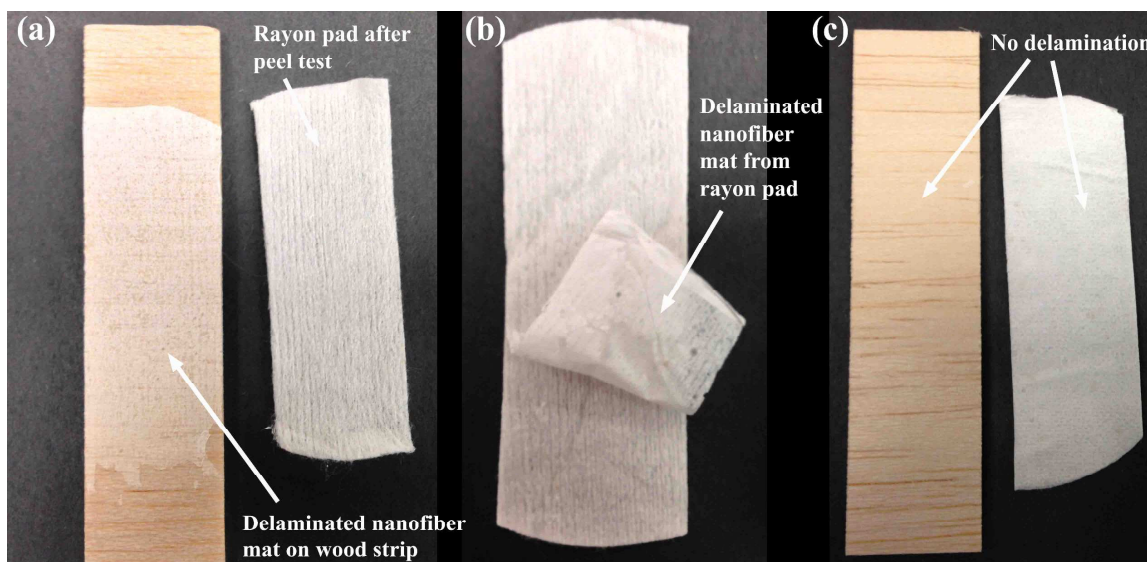


**Fig. 6.** (a) Delamination of soy protein/PCL fiber mat on wood strip. (b) Delamination from rayon pad, and (c) No delamination seen after prior electrospaying.

Subsequently, different samples of adhesive/soy protein/PVA and adhesive/soy protein/PCL fiber mats were pressed to balsa wood strips, and peeling tests were conducted after rolling 20 times 1 kg weight on the samples as described in the previous section. To achieve an accurate result, 10 samples of each kind were tested. Fig. 7a shows the average peel forces for the different adhesive/soy protein/PVA and adhesive/soy protein/PCL fibers compared with those of pure soy protein/PVA (sample PVA2-10) and pure soy protein/PCL (sample PCL1-10) nanofiber mats. For either of the two types of

soy protein/polymer fiber mat, the peel force was almost negligible for fiber mat without adhesive (samples PVA2-10 and PCL1-10). The peel force was the highest for PVAc wood glue (samples PVA2-AD3-10 and PCL1-AD3-10), followed by SIMALFA adhesive (samples PVA2-AD4-10 and PCL1-AD4-10), and the lowest for FDA adhesive (samples PCL1-AD1-10 and PCL1-AD1-10). The peel force for soy protein/PCL fibers with adhesives was more than the peel force for the corresponding soy protein/PVA fibers with the same adhesive (cf. Table 3). This is because adhesive was initially electrospayed for 5 min on bare rayon pad prior to electrospinning of PCL-based adhesive solutions. Hence, the total adhesive on the rayon pad comprised of both the electrospayed adhesive and the electrospun nanofibers with adhesives for the PCL-based samples was higher as compared to the adhesive content of the only-electrospun fibers with adhesives for the PVA-based samples.

The normal specific adhesive energy,  $G_n$  of the adhesive was calculated as,

$$G_n = \frac{F}{2W} \quad (1)$$

where  $F$  is the peel force and  $W$  the sample width. Eqn (1) is derived using the fact that work of the peel force is distributed between elastic storage and surface energy, as is usually done for adhesive joints when methods of fracture mechanics are applied<sup>50-52</sup>. Here, the sample width  $W$  was 2 cm for all samples. The thickness of the sample,  $t$  varied with different types of fiber mats. The thickness  $t$  of the sample was found by measuring the distance between the top layer of fibers and the base substrate of rayon pad using optical microscope Olympus BX-51. This was done by focusing first on the uppermost nanofiber layer and then on the bottommost nanofiber located on the rayon pad substrate.

The thickness of fiber mat for PVA-based solutions was found to be the same for 10 min of electrospinning and did not depend on the adhesive present in the solution. In other words, it can be concluded that the fiber mat thickness was determined by PVA and soy protein alone and was independent of the nature of the adhesive. The thickness,  $t$  was 280  $\mu\text{m}$  for samples PVA2-10, PVA2-AD1-10, PVA2-AD3-10, and PVA2-AD4-10. Due to the initial electrospinning of adhesives for PCL-based solutions, the thickness of the samples varied for different adhesives. The thicknesses of the samples were 375  $\mu\text{m}$ , 380  $\mu\text{m}$ , 310  $\mu\text{m}$ , and 315  $\mu\text{m}$  for PCL1-10, PCL1-AD1-10, PCL1-AD3-10, and PCL1-AD4-10, respectively. Electrospinning of adhesive AD1 led to formation of larger droplets on the bare rayon pad, thereby increasing the entire sample thickness significantly as compared to adhesives AD3 and AD4, which formed fine small droplets.

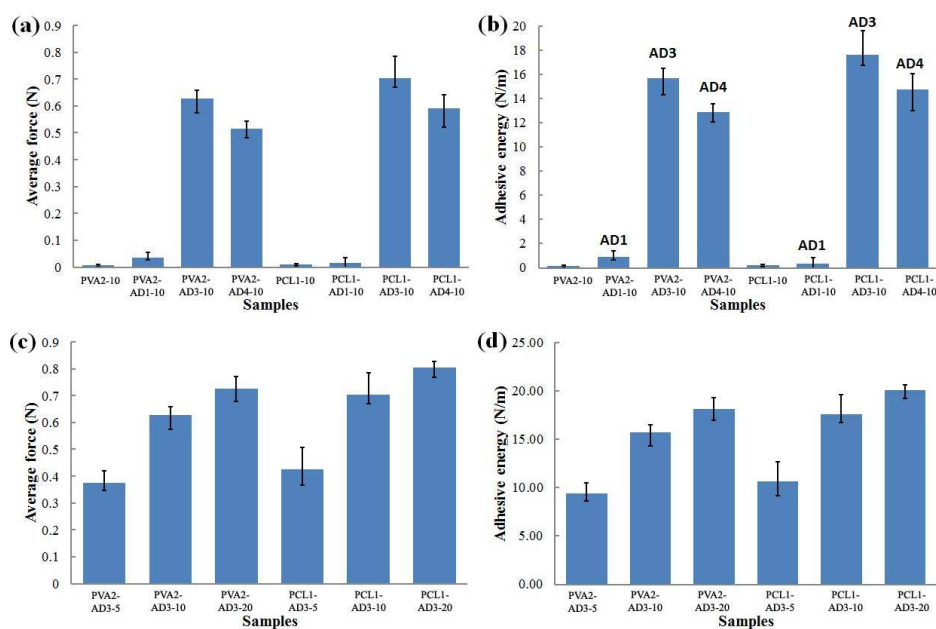


**Fig. 7.** (a and c) Peel force, and (b and d) normal specific adhesive energy of different samples.

**Table 3.** Peel force and normal specific adhesive energy of monolithic adhesive/soy protein/PVA and adhesive/ soy protein/PCL fibers.

Soy protein/PVA			Soy protein/PCL		
Sample	Peel force [N]	Normal specific adhesive energy [N/m]	Sample	Peel force [N]	Normal specific adhesive energy [N/m]
PVA2-10	0.0009	0.0225	PCL1-10	0.0025	0.0625
PVA2-AD1-10	0.0062	0.155	PCL1-AD1-10	0.0144	0.36
PVA2-AD3-10	0.6290	15.725	PCL1-AD3-10	0.7042	17.605
PVA2-AD4-10	0.5151	12.878	PCL1-AD4-10	0.5916	14.79

The normal adhesive energies  $G_n$  of different adhesives are listed in Table 3. The specific adhesive energy of should be considered as a material property for samples electrospun during the same time. Indeed, the electrospinning time controls the mat porosity and thus the number of contacts with the underlying surface<sup>53</sup>, which affects the specific adhesive energy together with the fiber and underlying materials. Accordingly, it was found that the specific adhesive energy obtained for the same adhesive using either soy protein/PVA or soy protein/PCL are, indeed, in the same range (cf. Fig. 7b and Table 3). Due to the presence of the initial electrospayed layer of adhesive, the peel force was higher for soy protein/PCL adhesive fibers than for soy protein/PVA fibers. Accordingly, the specific adhesive energy was also slightly higher for soy protein/PCL adhesive fibers.

Using eqn (1), we thus obtained the normal specific adhesive energy of different samples to be in the same range.

### 3.2.2 Effect of electrospinning time on normal specific adhesive energy of fiber mats

As mentioned above, the electrospinning time determines the mat porosity and thus the number of contacts with the underlying surface, which, in turn, affects the specific adhesive energy along with the fiber and underlying materials. Solutions PVA2-AD3 and PCL1-AD3 were electrospun for 5 min, 10 min and 20 min to study the dependence of the normal specific adhesive energy of the fiber mats on electrospinning time. As discussed in the previous section, fibers containing adhesive AD3, PVAc wood glue, possessed the maximum specific adhesive energy. Hence, the strongest adhesive was chosen to study the effect of electrospinning time on the normal specific adhesive energy. Though the thickness of the fiber mat increased with increasing electrospinning time, it did not increase proportionally to time. In other words, the thickness of fiber mat after 10 min of electrospinning was not doubled compared to that obtained in 5 min of electrospinning. Similarly, after 20 min of electrospinning, the thickness was neither 4 times that after 5 min of electrospinning, nor double that in 10 min of electrospinning. This proves that with longer electrospinning time, there were more fibers in the same layer and the distance between neighboring fibers, or the pore size, reduced. This increased the number of contacts of nanofibers with the underlying surface, and thus increased the peel force and the adhesive strengths of the samples. The thicknesses of the fiber mats measured using the optical microscope were 170  $\mu\text{m}$ , 280  $\mu\text{m}$ , 340  $\mu\text{m}$ , 195

$\mu\text{m}$ , 310  $\mu\text{m}$ , and 370  $\mu\text{m}$  for PVA2-AD3-5, PVA2-AD3-10, PVA2-AD3-20, PCL1-AD3-5, PCL1-AD3-10, and PCL1-AD3-20, respectively. The thickness of PCL-based fiber mat was larger than that of PVA-based fiber mat due to the prior electrospaying of adhesive on bare rayon pad.

Figs. 7c and 7d shows the peel forces and specific adhesive energy of samples PVA2-AD3-5, PVA2-AD3-10, PVA2-AD3-20, PCL1-AD3-5, PCL1-AD3-10, and PCL1-AD3-20. The peel force and the specific adhesive energy increases with increasing electrospinning time for both PVA- and PCL-based samples.

### 3.2.3 Shear specific adhesive energy of fiber mats

The results of the dead weight tests with the pure soy/polymer fiber mats and adhesive/soy/polymer fiber mats are listed in Table 4. From the weight measurements, the shear specific adhesive energy were calculated as

$$G_{\text{sh}} = \frac{mg}{2W} \quad (2)$$

where  $m$  is the mass of water in the container when the sample delaminated,  $g$  is gravity acceleration and  $W$  is the sample width. All dead weight tests were conducted with 2.3 cm x 5 cm samples, so the sample width was constant at 2.3 cm. Eqn (2) is derived similarly to eqn (1).

The shear specific adhesive energy  $G_{\text{sh}}$  measured with different adhesives are listed in Table 4. Similarly to the normal specific adhesive energy, the shear specific

adhesive energy obtained for the same adhesive using either soy protein/PVA or soy protein/PCL are in the same range (cf. Table 4). Due to the presence of the initial electrospayed layer of adhesive, the weight required to delaminate the samples was higher for soy protein/PCL adhesive fibers than for soy protein/PVA fibers. Since the area of the samples was the same for all the dead weight test samples, the higher weight for the adhesive/soy/PCL samples resulted in the higher adhesive forces. Also, similar to the results obtained in the normal adhesion test, the PVAc wood glue was the strongest and revealed the highest specific adhesive energy among the other adhesives tested.

**Table 4.** Dead weights and shear specific adhesive energy of monolithic adhesive/soy protein/PVA and adhesive/ soy protein/PCL fibers.

Soy protein/PVA			Soy protein/PCL		
Sample	Dead weight [g]	Shear adhesive specific energy [N/m]	Sample	Dead weight [g]	Shear adhesive specific energy [N/m]
PVA2-10	6.5	1.386	PCL1-10	14.3	3.049
PVA2-AD1-10	29.8	6.355	PCL1-AD1-10	54.1	11.537
PVA2-AD3-10	467.2	99.635	PCL1-AD3-10	594.6	126.805
PVA2-AD4-10	344.5	73.468	PCL1-AD4-10	405.6	86.498

The comparison of the results in Tables 3 and 4 shows that the shear specific adhesive energies can be significantly higher (typically by one or even two orders of

magnitude) than the normal specific adhesive energies of the corresponding fiber samples.

### 3.3 Electrospaying adhesive onto soy protein/PVA and soy protein/PCL nanofiber mats

A pristine soy protein/PVA fiber mat, sample PVA1-10, is shown in Figs. 8a and 8b. In Fig. 8a, the black thicker filaments are the background rayon fiber strands. Figs. 8c and 8d show the adhesive barrel-shaped drops on soy protein/PVA nanofibers after sample PVA1-10 had been electrospayed by adhesive AD2 for 10 min. Similarly, electrospaying of adhesives AD1 and AD2 was conducted for 10 min onto sample PCL1-10, as described in the experimental section. The electrospayed droplets have diameters in the range 1 – 10  $\mu\text{m}$ <sup>54</sup>. It should be emphasized that the adhesive droplets are located on the nanofibers and do not block the fiber pores. Fig. 9(1) illustrates SEM images of the soy protein/PVA fibers before and after the 180° peeling test of samples SPv01 and SPv02. Adhesive AD1 is a pressure-sensitive adhesive and the normal specific adhesive energy of samples SPv01 and SPc01 were tested for different applied pressures. The adhesive droplets were smeared onto the soy protein/PVA and soy protein/PCL nanofiber mats. Morphologically, for lower load (1 kg), the overall nanofiber structure remained intact even after the peeling test [compare Fig. 9(1)c with Fig. 9(1)b]. However, on application of a higher load (11.5 kg), the adhesive was completely smeared and the pore structure was lost with dramatically reduced pores [Fig. 9(1)d]. For reusability of the prepared nanofiber patches using repositionable adhesive

AD2, (samples SPv02 and SPc02), the normal specific adhesive energy of the samples were tested by repeating the loading-peeling test on the same sample. On repeating the peeling test on the same sample, some of the adhesive droplets coalesced [compare Fig. 9(1)g with Fig. 9(1)f]. After repeating the peeling test on the same sample seven times for sample SPv02, the adhesive drops were completely smeared [Fig. 9(1)h]. However, the pores, though diminished, were still not completely blocked. Fig. 9(2) shows the SEM images of adhesives electrospayed on separate samples of PCL-10. The peeling test for the same sample of SPc02 could be done only three times. This is because at the end of the third test, there was no adhesive remaining in the fiber mats and they could not be stuck again onto the balsa wood strip.

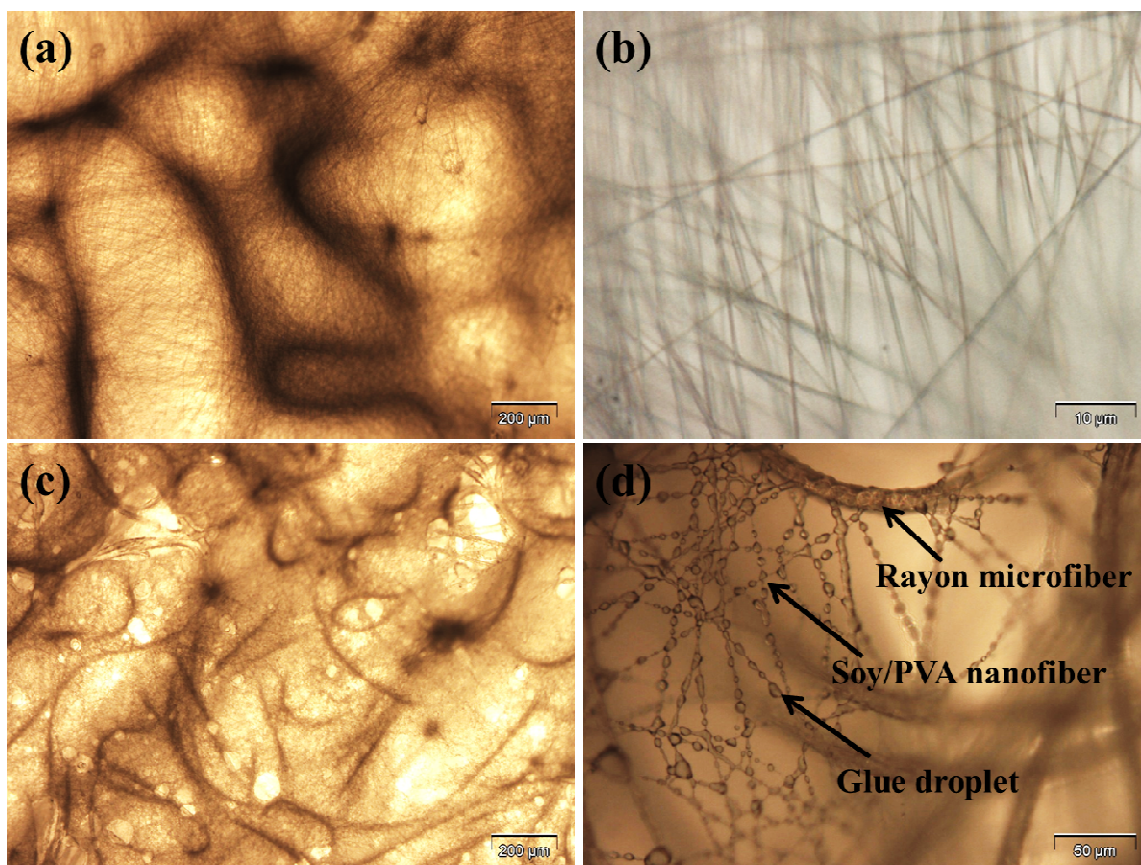


**Fig. 8.** Optical microscope images of: (a) As-deposited soy protein/PVA nanofibers on a rayon pad (sample PVA01-10); (b) Magnified view of panel (a); (c) Sample SPv02 with electrospayed adhesive droplets of repositionable adhesive AD2 on soy protein/PVA nanofiber mat; (d) A magnified view of panel (c).

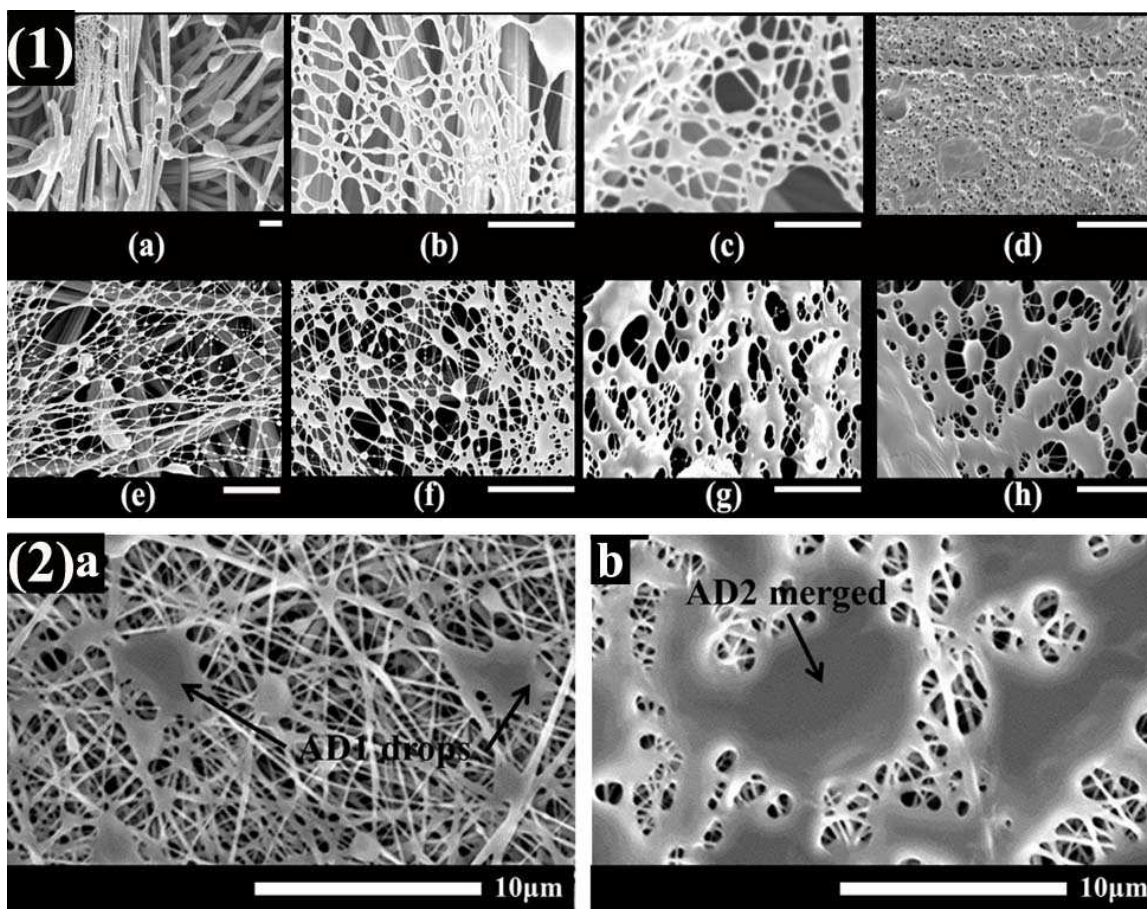


**Fig. 9.** (1) SPv01 before peeling test at: (a) Low magnification, and (b) Higher magnification. The samples after the peeling test with application of: (c) 1 kg load, and (d) 11.5 kg load. SPv02 sample before the peeling test at: (e) Low magnification, and (f) higher magnification. The samples after: (g) A single peeling test, and (h) after seven

consecutive peeling tests of the same sample. The scale bars are 50  $\mu\text{m}$ . (2) Electrospayed adhesives on soy protein/PCL fiber mats: (a) SPc01, and (2) SPc02.

The average peel force values for the 180° peeling tests of several samples are shown in Fig. 10. For pressure-sensitive adhesive AD1, increasing pressure leads to an increase in the average peel force (Fig. 10a for SPv01, and Fig. 10b for SPc01) required to peel the samples off. For repositionable adhesive AD2 in consecutive peeling tests (seven for SPv02, and three for SPc02 on the same sample) the results are shown in Figs. 10d and 10e, respectively. The peel force decreases from the maximal value after the first peeling test (from 0.1 N to 0.03 N), and thereafter remains in the range of 0.02 N to 0.05 N (Table 6).

The normal specific adhesive energy  $G_n$  of the adhesives was calculated using eqn (1). The thicknesses of the adhesive droplet layers on the soy protein/PVA nanofiber mats were as follows: for SPv01 the thickness was 92  $\mu\text{m}$ , for SPv02 the thickness was 27.7  $\mu\text{m}$ , for SPc01 the thickness was 303.3  $\mu\text{m}$ , and for SPc02 the thickness was 343.8  $\mu\text{m}$ . The sprayed adhesive layer was thicker for soy protein/PCL samples as compared to soy protein/PVA samples. This is due to the different material properties of the fibers. For hydrophobic PCL, the water soluble adhesive droplets were hanging from the fiber surfaces, whereas for hydrophilic PVA, the adhesive droplets were spread almost uniformly along the entire surface of the fibers. The adhesive energies along with the corresponding peel forces measured for different pressures applied on SPv01 and SPc01

samples and in consecutive peeling tests of the same samples of SPv02 and SPc02 are listed in Tables 5 and 6, respectively.

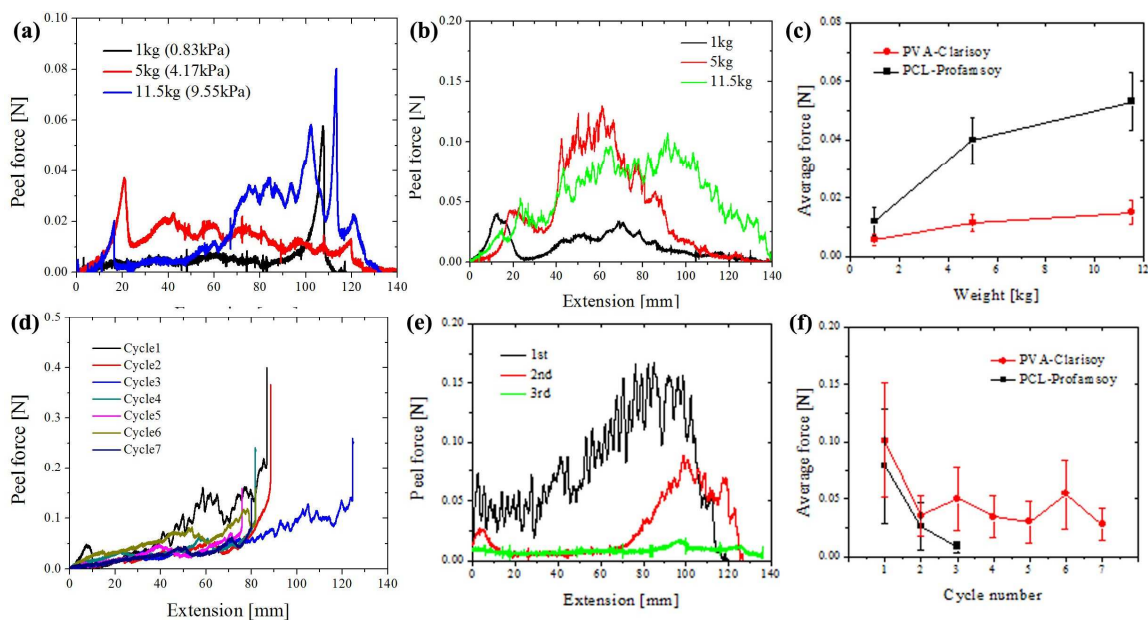


**Fig. 10.** Peel force for electro sprayed adhesive AD1: (a) sample SPv01, (b) sample SPc01, and (c) comparison between the two samples. Similar peel force graphs for adhesive AD2: (d) sample SPv02, (b) sample SPc02, and (c) comparison between the latter two samples.

**Table 5.** Peel force and normal specific adhesive energy of electro sprayed pressure-sensitive Micronax adhesive (AD1) for different applied pressures on samples SPv01 and SPc01.

	Sample SPv01		Sample SPc01	
Applied pressure [kPa]	Peel force [N]	Normal specific adhesive energy [N/m]	Peel force [N]	Normal specific adhesive energy [N/m]

0.83	0.00565	0.14	0.01188	0.25
4.17	0.01142	0.29	0.03982	0.83
9.55	0.01508	0.38	0.05312	1.11

**Table 6.** Peel force and normal specific adhesive energy of electro sprayed repositionable glue (AD21) for consecutive peeling tests of the same samples SPv02 and SPc02.

Cycle	Sample SPv02		Sample SPc02	
	Peel force [N]	Normal specific adhesive energy [N/m]	Peel force [N]	Normal specific adhesive energy [N/m]
1	0.10115	2.53	0.07901	1.65
2	0.03537	0.89	0.02624	0.55
3	0.05008	1.25	0.00844	0.18
4	0.03462	0.87	-	-
5	0.03022	0.76	-	-
6	0.05442	1.36	-	-
7	0.02774	0.69	-	-

Figs. 10c and 10f show the difference in the effect of the same adhesive electro sprayed on two different types of fiber mats. This can be explained as follows. Soy protein/PVA fibers (sample PVA1-10) are water soluble and hydrophilic in nature. The electro spraying conditions of the adhesives AD1 and AD2 were different, with AD1 producing large droplets and AD2 producing smaller ones. Accounting for the fact that the large droplets of AD1 contained more water, implies that impinging of these droplets onto PVA1-10 dissolved some of the fibers [Fig. 9(1)a]. The fiber morphology was lost in these places and adhesiveness was not found, accordingly. Soy protein/PCL sample

(PCL1-10) is insoluble in water. Hence, the size of the droplets did not affect the fibers and the adhesive drops were still located on the fiber mat [Fig. 9(2)a]. Therefore, with pressure-sensitive FDA-approved adhesive AD1, the peel force was higher for sample SPc01 as compared to sample SPv01 (Fig. 10c and Table 6). Due to an increase in the thickness of the adhesive layer for SPc01, there was no significant increase in the normal specific adhesive energy of the adhesive AD1 as compared to that of adhesive AD2.

The adhesive droplets of AD2 reaching soy protein/PVA mat were small and contained no water. Hence, the fiber morphology of the sample SPv02 remained unchanged [Fig. 9(1)e]. On the other hand, PCL is hydrophobic, and the small adhesive droplets could be easily detached from the sample (sample SPc02). Hence, on repetitive peeling of the same sample of SPc02, the adhesive droplets no longer remained on the fiber surface and almost no adhesive remained after peeling the same sample thrice (Fig. 10f).

### 3.4 Shear adhesion test

Tables 7 and 8 show the results of the dead weight test for the different samples prepared by electro spraying adhesives AD1 and AD2, respectively. The shear specific adhesive energy was calculated using eqn (2), with the samples having the same dimensions of 2.3 cm x 5 cm. The shear specific adhesive energy depends on both the type of the fibers and the adhesive. Comparing between samples SPc01 and SPv01 in Fig. 11a, it is seen that the sprayed AD1 solution is adhered better on PCL fibers than on PVA fibers. This is because the electro sprayed adhesive AD1 produced large droplets which

dissolved some of the soy/PVA fibers, whereas soy/PCL fibers being insoluble in water, remained intact. With the adhesive solution AD2, sample SPv02 shows the best shear specific adhesive energy in the first trial (see Fig. 11). Since the adhesive AD2 is repositionable, the same sample was used for repeated tests and the specific adhesive energy was found to drop dramatically in these tests. This happened because most of the sprayed adhesive was detached from the fiber surface after the first test. As mentioned above, PCL is not a water-soluble polymer, so water squeezed from the adhesive onto the fiber mat does not pose a problem. The investigation of the effect of glue on the shear specific adhesive energy of samples SPc01 and SPc02 (see Fig. 11a) revealed that AD1 possess a higher specific adhesive energy than AD2. The reason for the reduced specific adhesive energy of sample SPv01 as compared to SPv02 is related to the fact that the PVA fibers can be dissolved by large electro sprayed droplets of AD1. This proves that the shear specific adhesive energy of composite depends on a proper combination of the fiber and adhesive pair more than on the ability of the adhesive itself. The average value of the shear specific adhesive energy for the developed patches is in the range of 7 N/m – 25 N/m. This is significantly smaller than the values reported in ref 55 where the specific adhesive energy of pure nylon fibers was measured. It should be emphasized that ref 55 employed aligned 50 nm nanofibers and reported 2.7 times stronger adhesion than that of a gecko feet.

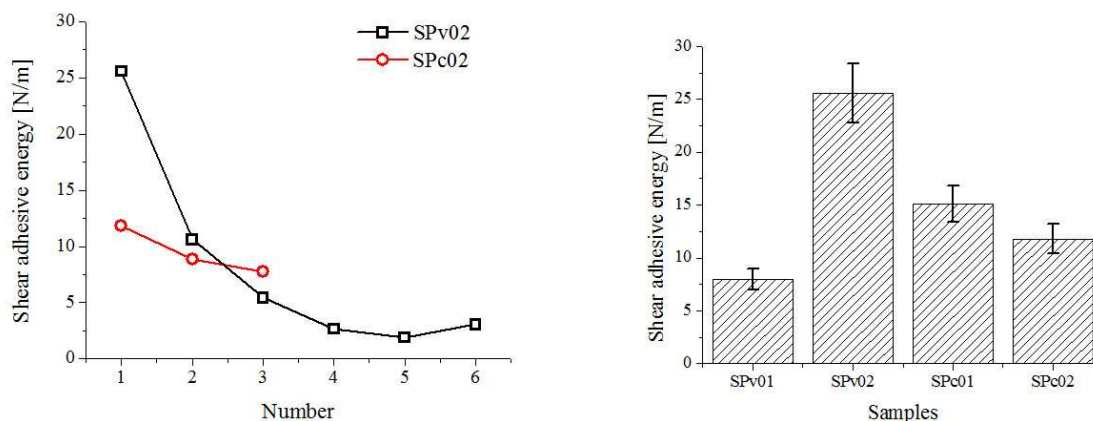


**Fig. 11.** (a) Shear specific adhesive energy in repeated test of SPv02 and SPc02. The horizontal axis reckons the number of the test in which the adhesive energy was measured, for example in test 4, the same sample has been stuck to the surface and removed for the 4<sup>th</sup> time. (b) Shear specific adhesive energy in the first test of SPv01, SPc01, SPv02 and SPc02 samples for the 0.83 kPa applied pressure.

**Table 7.** Dead weight and shear specific adhesive energy of electrospayed pressure-sensitive Micronax adhesive (AD1) for different applied pressures on samples SPv01 and SPc01.

Applied pressure [kPa]	Sample SPv01		Sample SPc01	
	Dead Weight[g]	Shear specific adhesive energy [N/m]	Dead Weight[g]	Shear specific adhesive energy [N/m]
0.83	37.4	7.98	70.6	15.1
4.17	108.8	23.2	183.5	39.1
9.55	146.0	31.1	289.3	72.4

**Table 8.** Dead weight and shear specific adhesive energy of electro sprayed repositionable glue (AD2) for consecutive peeling test of the same samples SPv02 and SPc02.

Cycle	SPv02		SPc02	
	Dead weight [g]	Shear specific adhesive energy [N/m]	Dead weight [g]	Shear specific adhesive energy [N/m]
1	120	25.6	55.3	11.8
2	49.7	10.6	41.5	8.85
3	25.4	5.43	36.4	7.75
4	12.4	2.65		
5	8.90	1.9		
6	14.3	3.05		

### 3.5 Compostability tests of the developed nanofiber patches

Compostability tests were conducted to test the longevity of the developed patches under atmospheric conditions. Fig. 12 shows the SEM images of the monolithic soy protein/PVA fibers (sample PVA2-10) and soy protein/PCL fibers (sample PCL1-10) taken immediately after electrospinning, 30 days after the sample was left open at room temperature and humidity, and after a water droplet was gently placed on the fiber mat. No degradation in the fiber structure was seen for sample PVA2-10 when left under open atmospheric conditions (Fig. 12b). However, with both the soy protein (Clarisoy) and PVA being water soluble, the entire fiber structure was lost on addition of a water droplet (Fig. 12c). With soy protein (Pro-Fam 955) and PCL, both being water insoluble, the

fibers remained intact under the atmospheric conditions, as well as on addition of water (Figs. 12e-f).

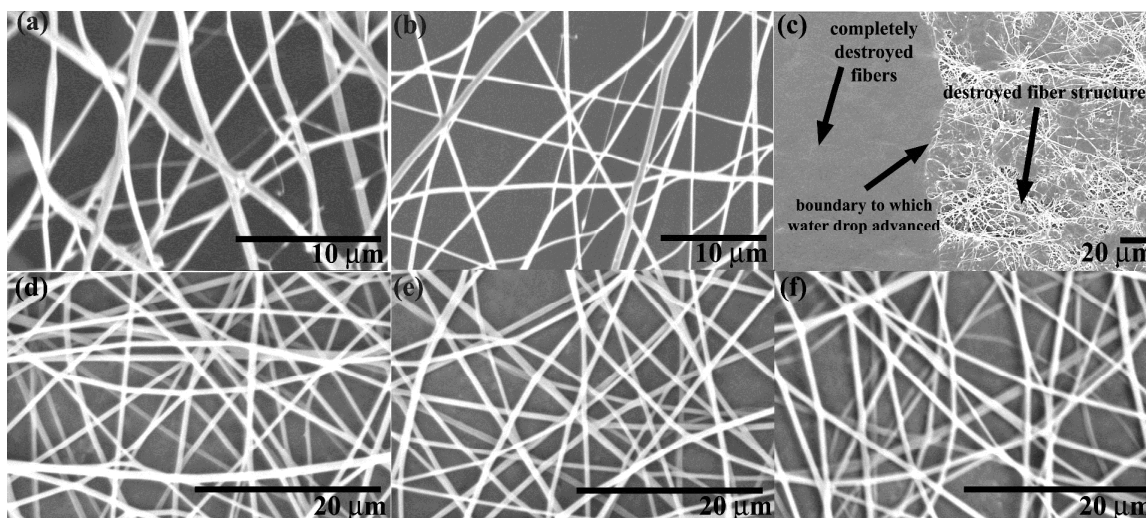


**Fig. 12.** Monolithic soy protein/PVA fibers: (a) Immediately after electrospinning, (b) 30 days after the fibers were left open under room temperature conditions, and (c) after addition of water droplet. Similar soy protein/PCL fibers: (d) immediately after electrospinning, (e) 30 days after the fibers were left under room temperature conditions, and (f) after addition of a water droplet.

PVA and PCL are two of the most biodegradable polymers used and their degradation rates depend on the environmental conditions rather than on the adhesives. In general, it takes several months for these polymers to degrade.<sup>56-59</sup> Grapevine pruning wounds, on the other hand, are susceptible to infection by fungi for as long as six to seven weeks<sup>60-62</sup>. Hence, the patches developed in the present work would remain intact until the plant wounds heal.

### 3.6 Use of sticky patches against esca

Practical application of the developed sticky nano-textured patches against esca attack and their sustainability under environmental conditions were assessed. The shear stress  $\tau_w$  on the patch surface was calculated using the Schultz-Grunow formula for the friction law in a turbulent boundary layer on a wall<sup>63</sup>

$$c_f = \frac{\tau_w}{\rho U^2 / 2} = \frac{0.370}{(\log_{10} Re_x)^{2.584}} \quad (3)$$

where  $c_f$  is the dimensionless friction coefficient,  $\rho$  is the air density,  $U$  is the wind velocity, and the Reynolds number  $Re=Ux/\nu$ , with  $x$  being the cross-section location, and  $\nu$  being the kinematic viscosity of air. For the estimate, take  $\rho = 1.177 \text{ kg/m}^3$ ,  $\nu = 0.15 \times 10^{-4} \text{ m}^2/\text{s}$ , and  $x=0.05 \text{ m}$ . The speed of air  $U$  is assumed as  $22.9 \text{ m/s}$ , the maximum speed at a California vineyard in April<sup>64</sup>. This wind speed is assigned as level 9 (strong gale) on the scale of 12 in Beaufort scale, which is sufficient enough to break off weak branches and twigs<sup>65</sup>. Then, eqn (3) yields  $\tau_w=1.9 \text{ Pa}$ . This stress is to be compared with the adhesive strength  $S_{sh} = mg / (W \times \ell) = 2G_{sh} / \ell$ . Using the values of  $G_{sh}$  listed in Tables 4, 7 and 8 and  $\ell = 5 \text{ cm}$  as in the experiments, we find that  $\tau_w$  is by several orders of magnitude smaller than  $S_{sh}$ . Therefore, the patches will not be blown off even by such a strong wind, even after the seventh cycle of loading.

## 4. Conclusions

Adhesive nanofiber patches were developed from monolithic soy protein/PVA and soy protein/PCL fibers and different water soluble adhesives. By varying the time of electrospinning, the pore sizes can be controlled, thereby a protective layer against fungi attack can be formed. These biodegradable and biocompatible nano-textured composite patches are radically different from the ordinary electrospun ultra-filtration membranes<sup>66,67</sup> and the void-free electrospun nanofiber composites<sup>68</sup>. The patches developed in the present work can be used to protect plants against fungi attack through prune locations and help preventing diseases like Vine Decline. The specific adhesive energies of the fibers were sufficient to withstand strong wind conditions, which mean that the patch stickiness makes them ready to be used on prune locations without being carried away by wind and allowing sufficient porosity for plants to breath. It should be emphasized that the normal specific adhesive energies between the nanofiber patches and wood measured in the present work (Tables 3, 5 and 6) are either close, or higher than the specific adhesive energies between two individual nylon 6 nanofibers measured using the in situ atomic force microscopy in ref 69 (0.427-0.613 N/m for two orthogonal fibers and 0.628 N/m for two parallel nanofibers). On the other hand, the shear specific adhesion energies measured in the present work (Tables 4, 7 and 8) are typically by one or two orders of magnitude higher than the normal specific adhesive energies measured in ref 69 and in the present work.

## Acknowledgment

This work was supported by a research contract with the United Soybean Board, Chesterfield, Missouri (research contract no. 1491).

## References

1. L. Mugnai, A. Graniti, and G. Surico, *Plant Disease*, 1999, **83**, 404-418.
2. M. Fischer and H. H. Kassemeyer, *Vitis-Geilweilerhof*, 2003, **42**, 109–116.
3. A. Graniti, *Phytopathologia Mediterranea*, 2006, **45**, 5-11.
4. W.D. Gubler and A. Eskalen, *Proc. 2nd Annual Nat'l Viticulture Research Conf.*, Jul 9–11, 2008.
5. D. T. O'Gorman, P. Haag and P. L. Sholberg, *Canadian plant disease survey, Inventaire des maladies des plantes au Canada*, 2008.
6. New Zealand winegrowers fact sheet, 2013.
7. <http://www.practicalwinery.com/mayjun01p14.htm>
8. A. L. Yarin, B. Pourdeyhimi and S. Ramakrishna, *Cambridge University Press, Cambridge*, 2014.
9. J. H. Wendorff, S. Agarwal and A. Greiner, *John Wiley and Sons, New York*, 2012.
10. Z. M. Huang, Y. Z. Zhang, M. Kotakic and S. Ramakrishna, *Compos Sci Technol.*, 2003, **63**, 2223-2253.
11. T. J. Sill and H. A. von Recum, *Biomaterials*, 2008, **29**, 1989-2006.
12. C. Y. Xu, R. Inai, M. Kotaki and S. Ramakrishna, *Biomaterials*, 2004, **25**, 877-886.

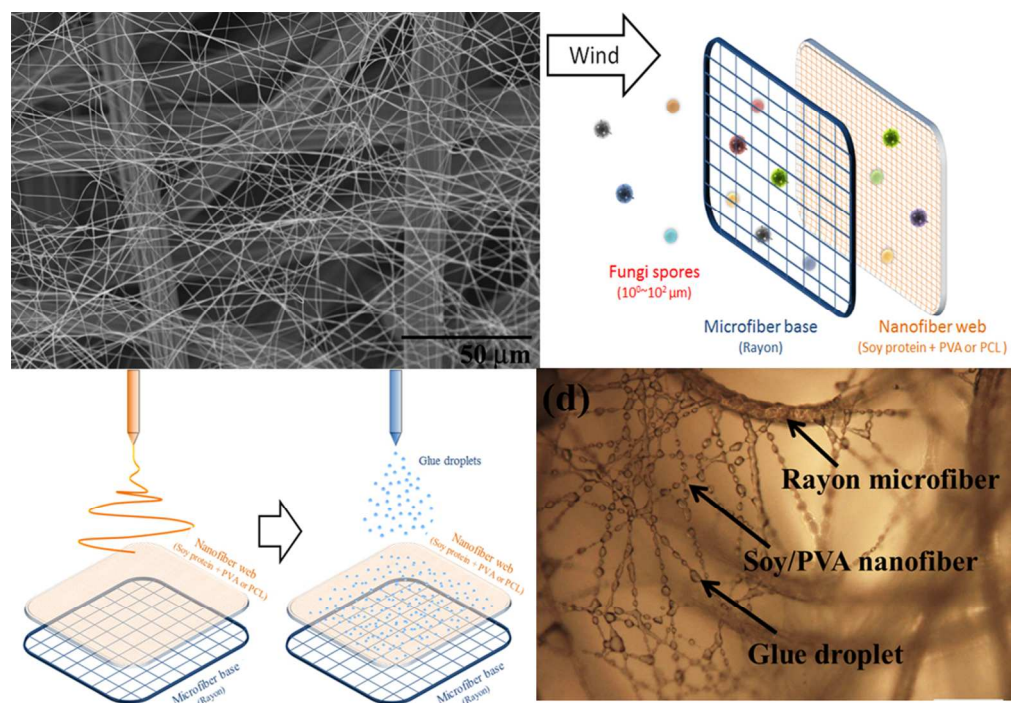
13. C. P. Barnes, S. A. Sell, E. D. Boland, D. G. Simpson and G. L. Bowlin, *Advanced drug delivery reviews*, 2007, **59**, 1413-1433.
14. J. R. Venugopal, S. Sridhar and S. Ramakrishna, *Plant Science Today*, 2014, **1(3)**, 151-154.
15. W. J. Li, R. Tuli, X. Huang, P. Laquerriere and R. S. Tuan, *Biomaterials*, 2005, **26**, 5158– 5166
16. J. Zeng, X. Xu, X. Chen, Q. Liang, X. Bian, L. Yang and X. Jing, *Journal of Controlled Release*, 2003, **92**, 227-231.
17. E. R. Kenawy, F. I. Abdel-Hay, M. H. El-Newehy and G. E. Wnek, *Materials Chemistry and Physics*, 2009, **113**, 296-302.
18. X. Hu, S. Liu, G. Zhou, Y. Huang, Z. Xie and X. Jing, *Journal of Controlled Release*, 2014, **185**, 12-21.
19. D. Bjorge, N. Daels, S. De Vrieze, P. Dejans, T. Van Camp, W. Audenaert, J. Hogie, P. Westbroek, K. De Clerck and S. W. H. Van Hulle, *Desalination*, 2009, **249**, 942-948.
20. M. Botes and T. E. Cloete, *Critical reviews in microbiology*, 2010, **36**, 68–81.
21. B. Ding and J. Yu (Editors), *Electrospun Nanofibers for Energy and Environmental Applications*, Springer, Berlin, **2014**.
22. S. Ramakrishna, R. Jose, P. S. Archana, A. S. Nair, R. Balamurugan, J. Venugopal and W. E. Teo, *Journal of materials science*, 2010, **45**, 6283-6312.
23. Q. Zhang, B. Damit, J. Welch, H. Park, C. Y. Wua and W. Sigmund, *J. Aerosol Sci*, 2010, **41**, 880-888.

24. S. Sundarrajan, K. L. Tan, S. H. Lim and S. Ramakrishna, *Procedia Engineering*, 2014, **75**, 159-163.
25. U. S. Sajeev, K. A. Anand, D. Menon and S. Nair, *Bulletin of Materials Science*, 2008, **31**, 343-351.
26. J. Zhao, L. Y. Guo, X. B. Yang, J. Weng, *Applied Surface Science*, 2008, **255**, 2942–2946.
27. Y. Mohammadi, M. Soleimani, M. Fallahi-Sichani, A. Gazme, V. Haddadi-Asl, E. Arefian, J. Kiani, R. Moradi, A. Atashi and N. Ahmadbeigi, *International Journal of Artificial Organs*, 2007, **30**, 204-211.
28. S. S. Zargarian and V. Haddadi-Asl, *Iranian Polymer Journal*, 2010, **19**, 457-468.
29. J. K. Wise, M. Cho, E. Zussman, A. L. Yarin, C. M. Megaridis and M. Cho, Electrospinning techniques to control deposition and structural alignment of nanofibrous scaffolds for cellular orientation and cytoskeletal reorganization. *Nanotechnology and Tissue Engineering*. 2<sup>nd</sup> Edition (eds. C.T. Laurencin and L.S. Nair). pp. 285- 303. *CRC Press, Boca Raton, CRC Press, Taylor and Francis*, **2014**.
30. J. Venugopal, P. Vadgama, T. S. S. Kumar and S. Ramakrishna, *Nanotechnology*, 2007, **18**, 055101.
31. T. Tanaka, T. Tsuchiya, H. Takahashi, M. Taniguchi and D. R. Lloyd, *Desalination* 2006, **193**, 367-374.
32. J. Huang, L. Zhang and F. Chen, *Journal of applied polymer science*, 2003, **88**, 3284-3290.

33. R. U. S. T. G. I. Chandra and R. Rustgi, *Progress in polymer science*, 1998, **23**, 1273-1335.
34. D. L. Kaplan, *Introduction to Biopolymers from Renewable Resources*, Springer, Heidelberg, **1998**.
35. S. Khansari, S. Sinha-Ray, A. L. Yarin and B. Pourdeyhimi, *Industrial & Engineering Chemistry Research*, 2013, **52**, 15104-15113.
36. S. C. Wong and J. F. Najem, *Polymeric fiber arrays for adhesion, ICF13*, **2013**.
37. H. Na, P. Chen, K. T. Wan, S. C. Wong, Q. Li and Z. Ma, *Langmuir*, 2012, **28**, 6677-6683.
38. F. M. Ballarin, T. A. Blackledge, C. Davis, L. Nicole, P. M. Frontini, G. A. Abraham and S. C. Wong, *Polymer Engineering & Science*, 2013, **53**, 2219-2227.
39. L. Sumin, D. Kimura, A. Yokoyama, K. Lee, J. C. Park and I. Kim, *Textile Research Journal*, 2009, **79**, 1085-1090.
40. L. Yao, T. W. Haas, A. Guiseppi-Elie, G. L. Bowlin, D. G. Simpson and G. E. Wnek, *Chem. Mater.*, 2003, **15**, 1860-1864.
41. S. L. Shenoy, W. D. Bates and G. Wnek, *Polymer*, 2005, **46**, 8990-9004.
42. Y. Zhang, M. W. Lee, S. An, S. Sinha-Ray, S. Khansari, B. Joshi, S. Hong, J. H. Hong, J. J. Kim, B. Pourdeyhimi, S. S. Yoon and A. L. Yarin, *Catalysis Communications*, 2013, **34**, 35-40.
43. L. V. Schueren, B. D. Schoenmaker, O. I. Kalaoglu and K. D. Clerck, *European Polymer Journal*, 2011, **47**, 1256-1263.

44. D. H. Reneker, A. L. Yarin, E. Zussman and H. Xu, *Adv. Appl. Mech.*, 2007, **41**, 43-195.
45. D. H. Reneker and A. L. Yarin, *Polymer*, 2008, **49**, 2387-2425.
46. A. Greiner, J.H.Wendorff, A.L. Yarin and E. Zussman, *Applied Microbiology and Biotechnology* 2006, **71**, 387-393.
47. A. L. Yarin, E. Zussman, J.H. Wendorff and A. Greiner, *J. Mater. Chem.* 2007, **17**, 2585-2599.
48. A.L. Yarin, *Polymers Advanced Technologies* 2011, **22**, 310-317.
49. S. Sinha-Ray, Y. Zhang, A. L. Yarin, S. C. Davis and B. Pourdeyhimi, *Biomacromolecules*, 2011, **12**, 2357-2363.
50. I. V. Obreimow, *Proc. Roy. Soc. Ser. A.*, 1930, **127**, 290-297.
51. B. M. Malyshev and R. L. Salganik, *Int. J. Fracture Mech.*, 1965, **1**, 114-128.
52. K. T. Wan and Y. W. Mai, *Int. J. Fracture*, 1995, **74**, 181-197.
53. R. P. Sahu, S. Sinha Ray, A. L. Yarin and B. Pourdeyhimi, *Soft Matter* 2012, **8**, 3957-3970.
54. K. Tang and A. Gomez *J. Colloid Interface Sci.*, 1995, **184**, 500-511.
55. J. F. Najem, S. C. Wong and G. Ji, *Langmuir*, 2014, **30**, 10410–10418.
56. X. Tang and S. Alavi *Carbohydrate Polymers*, 2011, **85**, 7-16.
57. D. Darwis, H. Mitomo and F. Yoshii *Polymer Degradation and Stability*, 1999, **65**, 279-285.
58. A. de Campos, J. C. Marconato and S. M. Martins-Franchetti *Brazilian Archives of Biology and Technology*, 2011, **54**, 1367-1378.
59. E. Rudnik *Compostable Polymer Materials*, Elsevier Science, Amsterdam, **2008**.

60. P. E. Rolshausen, J. R. Urbez-Torres, S. Rooney-Latham, A. Eskalen, R. J. Smith and W. D. Gubler *Journal of Enology and Viticulture*, 2010, **61.1**, 113-119.
61. W. D. Gubler, P. E. Rolshausen, F. P. Trouillas, J. R. Urbez and T. Voegel *Practical Winery and Vinetard Magazine*, Jan 2005.
62. A. Eskalen, A. J. Feliciano and W. D. Gubler *Plant Disease*, 2007, **91.9**, 1100-1104.
63. S. B. Pope, *Cambridge University Press, Cambridge*, **2000**.
64. <http://www.usa.com/vineyard-ca-weather.htm>
65. <http://www.unc.edu/~rowlett/units/scales/beaufort.html>
66. K. Yoon, K. Kim, X. Wang, D. Fang, B. S. Hsiao and B. Chu, *Polymer*, 2006, **47**, 2434-2441.
67. R. Balamurugan, S. Sundarrajan and S. Ramakrishna, *Membranes*, 2011, **1**, 232-248.
68. U. Stachewicz, F. Modaresifar, R. J. Bailey, T. Peijs and A. H. Barber, *Applied Materials & Interfaces*, 2012, **4**, 2577-2582.
69. U. Stachewicz, F. Hang and A. H. Barber, *Langmuir*, 2014, **30**, 6819-6825.



106x73mm (255 x 255 DPI)